Inhibition of Grb2 SH2 Domain Binding by Non-Phosphate-Containing Ligands. 2. 4-(2-Malonyl)phenylalanine as a Potent Phosphotyrosyl Mimetic†

Yang Gao,[‡,+] Juliet Luo,[§,+] Zhu-Jun Yao,[‡] Ribo Guo,[§] Hong Zou,[§] James Kelley,[‡] Johannes H. Voigt,[‡] Dajun Yang,[§,¶] and Terrence R. Burke, Jr.*[,‡,¶]

Laboratory of Medicinal Chemistry, Division of Basic Sciences, National Cancer Institute, National Institutes of Health, Bethesda, Maryland 20892, and Lombardi Cancer Center, Georgetown University Medical Center, Washington, DC

Received August 20, 1999

Nonhydrolyzable phosphotyrosyl (pTyr) mimetics serve as important components of many competitive Grb2 SH2 domain inhibitors. To date, the most potent of these inhibitors have relied on phosphonate-based structures to replace the 4-phosphoryl group of the parent pTyr residue. Reported herein is the design and evaluation of a new pTyr mimetic, *p*-malonylphenylalanine (Pmf), which does not contain phosphorus yet, in Grb2 SH2 domain binding systems, approaches the potency of phosphonate-based pTyr mimetics. When incorporated into high affinity Grb2 SH2 domain-directed platforms, Pmf is 15−20 times more potent than the closely related previously reported pTyr mimetic, *O*-malonyltyrosine (OMT). Pmf-containing inhibitors show inhibition constants as low as 8 nM in extracellular Grb2 binding assays and in whole cell systems, effective blockade of both endogenous Grb2 binding to cognate erbB-2, and downstream MAP kinase activation. Evidence is provided that use of an N^{α}-oxalyl auxiliary enhances effectiveness of Pmf and other inhibitors in both extracellular and intracellular contexts. As one of the most potent Grb2 SH2 domain-directed pTyr mimetics yet disclosed, Pmf may potentially have utility in the design of new chemotherapeutics for the treatment of various proliferative diseases, including breast cancer.

Introduction

Protein-tyrosine kinases (PTKs) serve as cornerstones for cellular signal transduction through creation of the phosphotyrosyl (pTyr, **1**) motif (Chart 1). By enzymatic addition of phosphate to tyrosyl residues, information is conveyed similar to "flipping a switch" or "converting a binary 0 to 1." Propagation of this information is achieved by the actions of protein tyrosine binding (PTB) and Src homology 2 (SH2) domains, whose binding affinities for tyrosyl-containing ligands can be reversed from low to high by introduction of the tyrosyl phosphate moiety.[3] SH2 domain inhibitors may potentially afford new approaches for the treatment of a variety of diseases, including several cancers, where SH2 domains frequently provide critical links between growth factor receptor PTKs and downstream Ras-proteins that have been implicated in oncogenic processes, including the ErbB-2 (HER-2/neu) PTK found in a large proportion of breast cancers.[4] There is a significant overexpression of mRNA for ErbB-2 in many breast cancers, with an associated increase in the levels of its phosphorylated gene product, p185erbB-2. Inhibitors of Grb2 SH2 domain binding could potentially uncouple p185erbB-2 from the Ras pathway and, in so doing, attenuate its transforming effects.[5,6] The possible therapeutic utility of Grb2 SH2 domain inhibitors has made their development an important area of research.[1,7−22]

Chart 1

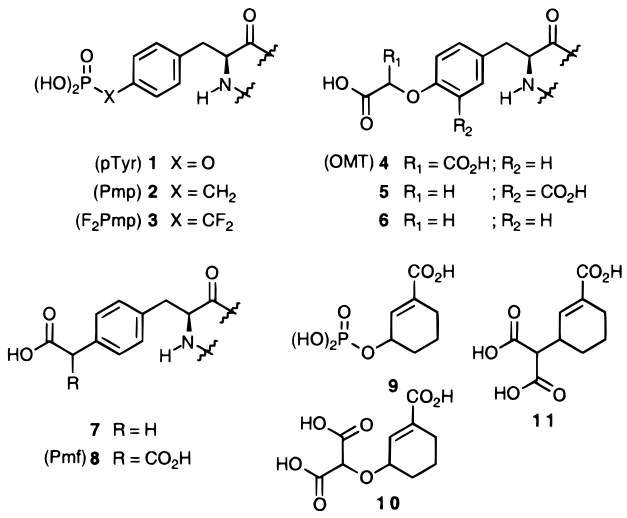

Although pTyr residues play central roles in ligand recognition and binding by SH2 domains, their hydrolytic lability to cellular phosphatases limits their utility for inhibitor design. For this reason, pTyr mimetics have become important tools for developing SH2 domain antagonists, with a particular emphasis on phosphate surrogates having been dictated by the essential role of the phosphate group in pTyr binding affinity.[23,24] For the Grb2 SH2 domain, the phosphate moiety undergoes key interactions with the Arg 67 and Arg 86 residues, as well as with a number of Ser side chain hydroxyls which line the pTyr binding pocket. Additional key

† For the previous paper in this series, see refs 1 and 2.

* To whom correspondence should be addressed. Mailing address: Building 37, Room 5C06, National Institutes of Health, Bethesda, MD 20892. Tel: (301) 496-3597. Fax: (301) 402-2275. E-mail: tburke@helix.nih.gov.

‡ National Cancer Institute.

§ Georgetown University Medical Center.

+ Authors contributed equally to the work.

¶ Senior authorship.

10.1021/jm9904248 CCC: $19.00
Published on Web 02/19/2000

Scheme 1

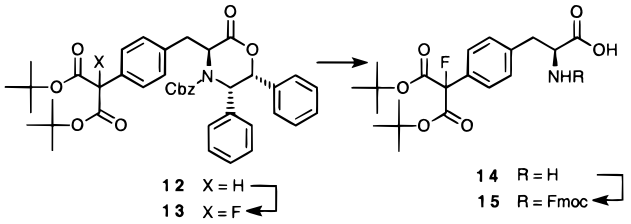

interactions occur between the Arg 67 residue and the carbonyl group of the pY-1 residue.[25−28] In light of the importance to overall affinity of interactions within the pTyr binding pocket, various ways of maintaining these without the use of phosphate groups have been examined.[23,24] Until recently, the most potent of these analogues have employed phosphonates of phenylalanine, in which the phosphoryl ester oxygen has been replaced either by a methylene (Pmp, **2**)[29] or by a substituted methylene (F_2Pmp, **3**).[30] Alternative compounds based on non-phosphorus-containing phosphate mimetics have generally been significantly less potent than phosphonates. Among such latter compounds are agents which utilize carboxyl groups to introduce the anionic oxygen functionality of the parent phosphate. Early carboxy-based pTyr analogues include *O*-(2-malonyl)tyrosine (OMT, **4**),[31] whose design was predicated on mimetics of 4,5-dideoxyshikimate-3-phosphate (**9**) that employed the malonyl group as a phosphate replacement in compounds such as **10** and **11**.[32] Of note was the loss of potency incurred in **11** by removal of the 2-malonyl ether oxygen. When incorporated as a pTyr replacement in high affinity Grb2 SH2 domain binding sequence, OMT exhibited a greater than 100-fold reduction in potency relative to the parent pTyr-containing peptide.[8] More recently the isomeric bis-carboxy analogue **5** as well as monocarboxy-based pTyr mimetics **6** and **7** have also demonstrated significantly reduced Grb2 SH2 domain binding potency relative to the parent pTyr-containing ligand.[1] Because carboxy-based compounds may potentially afford pharmacologically interesting alternatives to phosphonate-based pTyr mimetics, developmental efforts have continued. Accordingly, herein is reported a new pTyr mimetic, *p*-(2-malonyl)phenylalanine (Pmf, **8**), which exhibits Grb2 SH2 domain binding potency approaching that of phosphonate-based mimetics.

Synthesis

All pTyr mimetics were utilized in the present study as their N^{α}-Fmoc derivatives, with orthogonal *tert*-butyl protection of hydroxyl-bearing side chain functionality. Except as indicated below, synthesis of these amino acid analogues have already been reported,[1,31,33−35] including that of the title compound, N^{α}-Fmoc 4-(bis((*tert*-butyl)-oxycarbonyl)methyl)-L-phenylalanine.[36] As shown in Scheme 1, fluoro-Pmf analogue **15** was prepared by electrophilic fluorination of iminolactone **12**[36] (NaH at room temperature followed by *N*-fluorobenzenesulfonimide),[37] followed by hydrogenolytic deprotection of the resulting α-fluoro **13** to give free amino acid **14**, which was then treated with Fmoc-OSu/Na_2CO_3. To determine the enantiomeric purity of final product **14**, a leucine amide dipeptide was prepared by solid-phase techniques, with HPLC separation of any resulting diastereomers then performed. Reference peptides were prepared using **14** and racemic D,L-leucine-amide resins. The resulting free amino-containing dipeptide amides showed good separation of diastereomers (diastereomeric retention time difference of 4 min). The procedure was then repeated using enantiomerically pure L-leucine-amide resin. Any observed diastereomeric contamination evident in this latter peptide would arise solely from **14**. Less than 3% enantiomeric impurity was observed, indicating at least 94% ee for title compound **14**. Synthesis of naphthyl-containing tripeptides **25**, **28**, and **29** was accomplished using Fmoc protocols similar to a recent report.[1] Coupling of free amine-containing **16** with appropriate protected amino acid analogues, yielded intermediates **17a**−**19a**, which were then N-terminally deprotected and converted to either their *N*-acetyl or *N*-(*tert*-butyl oxalyl) derivatives (Scheme 2). Removal of carboxylic *tert*-butyl protection (TFA) yielded the desired final compounds **25**, **28**, and **29**. In a similar fashion, 5-methylindolyl-containing compounds **30** and **31** were prepared starting from asparagine amide **20**[19] following conversion to dipeptide **21**. All final products were purified by HPLC (Scheme 3).

Scheme 2

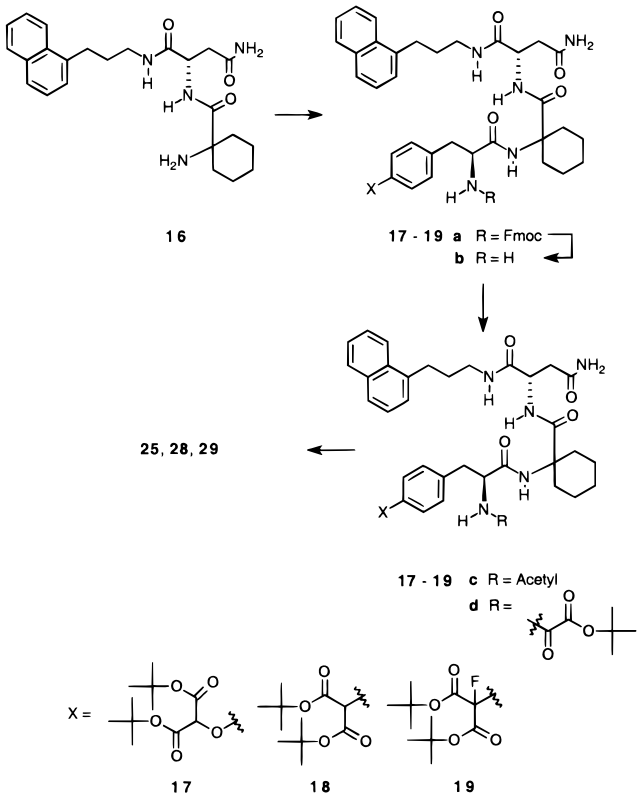

Results and Discussion

Inhibition of Grb2 SH2 Domain Binding in Extracellular ELISA Assays. For Grb2 SH2 domain inhibitors, the importance to overall affinity of interactions within the pTyr binding pocket has resulted in efforts to maintain high affinity without reliance on hydrolytically labile phosphate functionality. Until recently, the most potent Grb2 SH2 domain-directed pTyr mimetics have relied on phosphonate-based structures such as Pmp (**2**),[1,7,19] with dicarboxy-based pTyr mimetics such as *O*-malonyltyrosine (OMT, **4**)[8] and the

Scheme 3

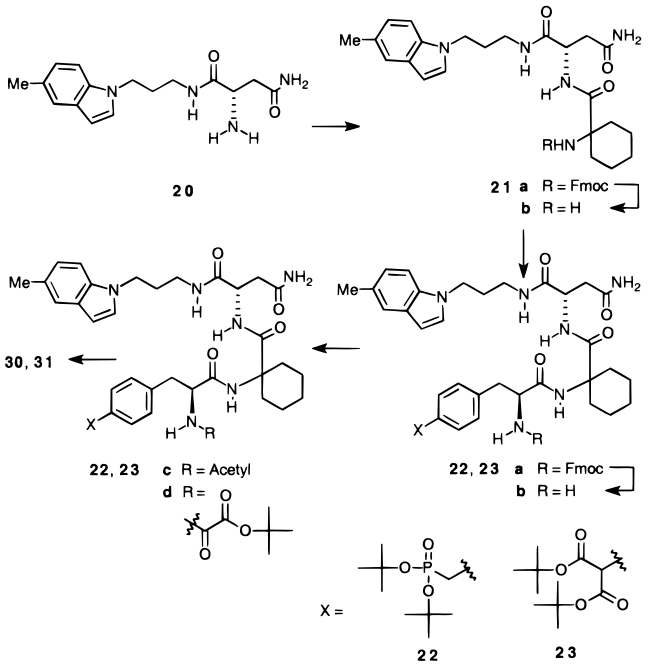

isomeric **5**[38] exhibiting much less affinity. In the present study, different arrangements of carboxyl groups were appended onto phenylalanyl residues in order to maintain anionic interactions with SH2 domain Arg67 and Arg86 residues, similar to those exhibited by the $O{=}P(O^-)_2$ groups of either pTyr or Pmp. Using a previously reported high affinity β-bend mimicking Grb2 SH2 domain binding platform,[14] we have examined the Grb2 SH2 domain binding potency of a series of pTyr mimetics. Each analogue was prepared in both its N^{α}-acetyl and N^{α}-oxalyl forms, predicated on our previous observations that the *N*-oxalyl derivatives typically exhibit greater binding potencies than their N^{α}-acetyl counterparts.[1,39] In the present study, N^{α}-oxalyl Pmp analogue **24b** (IC_{50} = 50 nM; Table 1) served as a reference, since Pmp is one of the most potent Grb2 SH2 domain-directed phosphorus-containing pTyr mimetics reported to date. Using an ELISA-based extracellular binding assay, the OMT residue (**4**) resulted in an approximate 20-fold loss of potency (compound **25b**; $IC_{50} = 1.1\ \mu M$) relative to the Pmp. Molecular dynamics simulations comparing the Grb2 SH2 domain binding of OMT and Pmp residues indicated that the OMT malonyl group extends farther out from the aryl ring than the phosphonate group which it mimics, resulting in a degree of misalignment (Figure 1a).

In contrast to the over-extension of carboxyls observed with OMT, a recent X-ray structure of the monocarboxy-based pTyr mimetic, carboxymethylphenylalanine (Cmf, **7**) bound to the $p56^{lck}$ SH2 domain, indicated good alignment of the carboxyl and phosphoryl oxygens while maintaining phenyl ring registry with the parent pTyr residue.[40] Indeed, molecular modeling dynamics simulations of the Cmf residue bound within the Grb2 SH2 domain similarly showed good registry of carboxyl oxygens as well as maintenance of phenyl ring registry when compared to Pmp.[39] Alternatively, in a fashion similar to that seen with OMT, the carboxymethyltyrosyl residue (Cmt, **6**) showed misalignment due to over-extension caused by the added carboxymethyl ether oxygen (Figure 1b). In agreement with this modeling data, ELISA data showed that Cmt-containing analogue **26b** (IC_{50} = 19 μM) was approximately 20-fold less potent than the corresponding Cmf-containing **27b** (IC_{50} = 1 μM).[39]

Table 1. Inhibition of Grb2 SH2 Domain Binding[a]

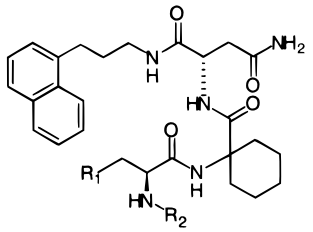

	R_2 = **a**	**b**
R_1	IC_{50} (μM)	
24	0.02 ± 0.01 (n = 3)[b]	0.05 ± 0.04 (n = 9)[b]
25	2.75 ± 0.64 (n = 3)	1.1 ± 0.14 (n = 3)
26	68[c]	19[c]
27	6.4[c]	1[c]
28	0.16 ± 0.02 (n = 4)	0.07 ± 0.04 (n = 11)
29	0.68 ± 0.58 (n = 3)	0.17 ± 0.13 (n = 3)

[a] Data were obtained using a Grb2 SH2 domain GST fusion protein in an ELISA assay as described in the Experimental Section. IC_{50} values were determined from serial dilutions of inhibitor with each concentration done in triplicate. Numbers in parentheses indicate the total number of ELISA experiments. [b] Plasmon resonance-based IC_{50} values have been reported previously (ref 1). [c] Single determinations were performed since results are similar to previously reported plasmon resonance-based IC_{50} values (ref 16).

Improvements in both predicted binding (Figure 1) and actual binding (Table 1) of Cmf (**7**) relative to Cmt (**6**) residues, induced by deletion of the bridging ether oxygen, led us to examine a similar modification of the OMT residue (**4**). This resulted in the new pTyr mimetic, *p*-malonylphenylalanine Pmf (**8**), which upon subjection to molecular modeling dynamics ligated to the Grb2 SH2 domain, compared favorably with a Pmp residue (Figure 1c). Subsequent ELISA binding analysis showed Pmf-containing **28b** (IC_{50} = 70 nM) to be approximately equipotent to Pmp (Table 1). These results indicated that removing the ether oxygen from OMT to give Pmf provided an approximate 15-fold increase in binding potency, resulting in one of the most potent non-phosphorus-containing pTyr mimetics yet reported for Grb2 SH2 domain binding. This finding is somewhat

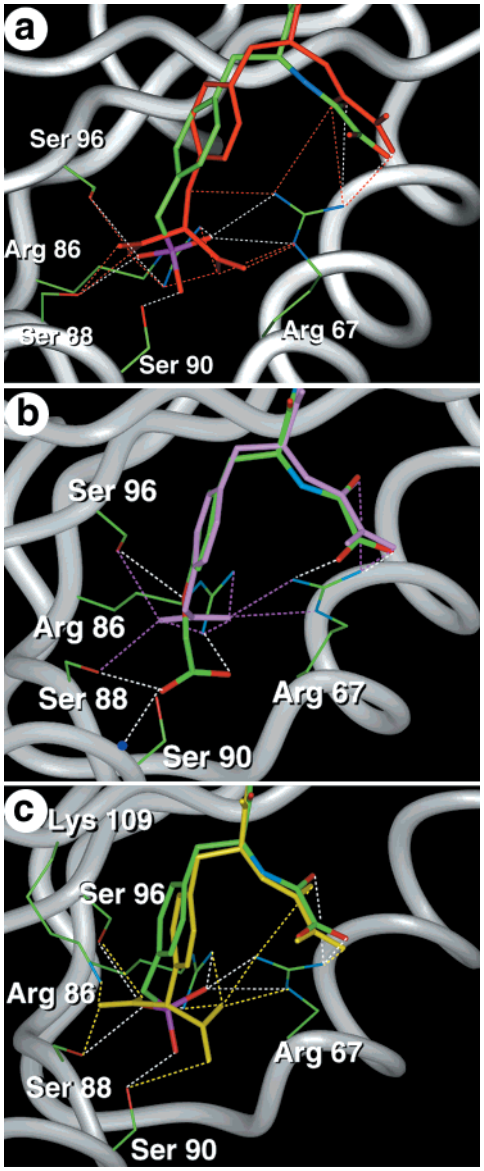

Figure 1. Comparison of the Grb2 SH2 domain ligand binding modes based on molecular modeling as described in the Experimental Section. Protein backbone atoms are superimposed. Heavy atoms of both ligands and one set of interacting side chains are shown in each panel. Dashed lines in ligand color, or white for ligands colored by atom type, show hydrogen bonds: (a) **24b** and **25b** (red); (b) **26b** and **27b** (magenta); (c) **24b** and **28b** (yellow).

counter to earlier uses of malonyl-based phosphate mimetics in 4,5-dideoxyshikimate-3-phosphate analogues, where removal of the ether oxygen from compound **10** significantly reduced potency (compound **11**).[32] To potentially compensate for the loss of hydrogen bonding functionality incurred by loss of the ether oxygen in Pmf, fluorine was introduced at the malonyl α-methylene in a modification similar to the previously reported synthesis of fluoromalonyltyrosine (FOMT).[37] This resulted in a reduction in potency (compound **29b**; IC_{50} = 170 nM), as was observed when carboxydifluoromethyl phenylalanine was prepared by addition of fluorines to Cmf.[34,39]

Whole Cell Assays: Intracellular Inhibition of Grb2 SH2 Domain Binding. ELISA data present in Table 1 and discussed above are from extracellular assays which measure inhibition of binding between

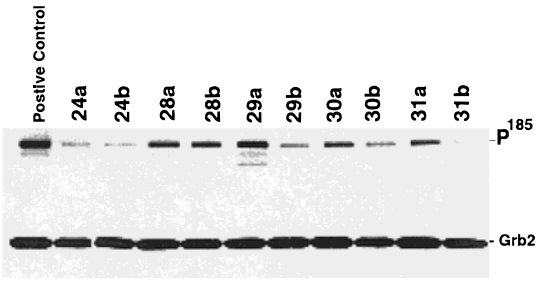

Figure 2. Effects of inhibitors on interaction of Grb2 with tyrosine phosphorylated p185 erbB-2 in human breast cancer cells MDA-MB-453 as described in the Experimental Section. MDA-MB-453 cells were plated in 100 mm dishes cultured in IME with 10% FBS medium overnight. Cells were treated with inhibitors (25 μM) for 3 h, washed, and lysed and 500 μg of protein immunoprecipitate was treated with Grb2 antibody. Co-immunoprecipitated pTyr-containing p185 erbB-2 was detected using pTyr antibody (Py99) and immunoblotting. Western blotting with Grb2 MAb was done as a control.

isolated Grb2 SH2 domain constructs and short pTyr-containing peptides. This type of data is a useful indicator of protein−inhibitor interaction. However, in physiological contexts, binding interactions occur between full Grb2 protein (which consists of an SH2 domain and two SH3 domains[41]) and phosphorylated proteins, which include Shc and erbB-2 growth factor receptor cytoplasmic domains. Therefore, effective inhibition by synthetic ligands in whole cell environments differs from extracellular ELISA assays in two ways: (1) In cellular systems ligands must cross cell membranes prior to interacting with targets, and (2) both the Grb2 SH2 domain host and cognate phosphorylated erbB-2 proteins, with which the inhibitors must compete, are much larger and more complex in the cellular system than in the ELISA assay. To obtain a more relevant measure of the inhibitory potency of synthetic ligands, binding experiments were therefore conducted in whole cells in which inhibition of binding of full length Grb2 to native erbB-2 was measured following treatment of cells with inhibitors. Shown in Figure 2 are results from these assays in which it is seen that inhibition of cognate Grb2 SH2 domain binding was observed with potencies varying roughly in the same rank order as that observed in the ELISA assays. Of note was the apparent ability of the N^{α}-oxalyl group to enhance cellular potency despite the added negative charge which it imparts. Although the N^{α}-oxalyl group enhances binding potency in extracellular ELISA assays, it would have been expected in cellular assays that the added charge could potentially hinder cell membrane penetration, thereby offsetting binding enhancement.

Intracellular Inhibition of MAP Kinase Activation. MAP kinase activation is a downstream event associated with erbB-2/Grb2 signaling through the Ras pathway, occurring distal to the Grb2-dependent activation of membrane-bound Ras. Therefore, measurement of inhibition of MAP kinase activation by exogenously administered Grb2 SH2 domain antagonists indicates the cumulative effectiveness of these agents in disconnecting the Ras pathway from erbB-2 signaling. In the present study, inhibition of MAP kinase was measured by MAP kinase specific antibody in MDA-MB-453 cells treated with growth factor heregulin (HRG). Experi-

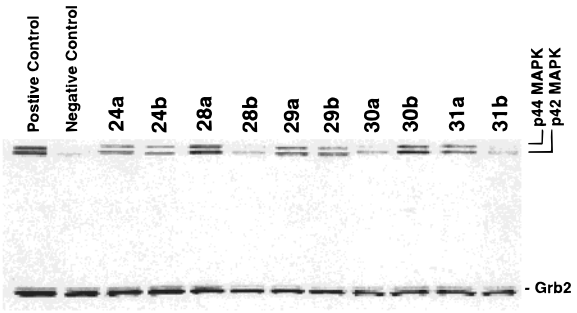

Figure 3. Effects of Grb2 inhibitors on activation of MAP kinase in human breast cancer cells MDA-MB-453 as described in the Experimental Section.

ments were repeated at least two times for all compounds, with representative results from active analogues shown in Figure 3. Inhibition of MAP kinase activation was observed in response to extracellular administration of Grb2 antagonists in a fashion approximating that seen both for extracellular ELISA binding (Table 1) and intracellular binding of Grb2 to p185erbB-2 (Figure 2). Of note was the general ability of N^{α}-oxalyl derivatives to elicit significantly greater inhibition than their N^{α}-acetyl counterparts, with Pmf-containing **28b** reducing MAP kinase activation to near basal levels when administered extracellularly at a concentration of 25 μM.

5-Methylindolyl Analogues. The focus of our efforts on the development of pTyr mimetics which can bind with high affinity in the Grb2 SH2 domain pTyr binding pocket has utilized the naphthyl-containing β-bend mimicking dipeptide construct **16** as a display platform previously disclosed by Furet et al. to exhibit high Grb2 SH2 domain affinity when N-terminally coupled to N^{α}-acetyl pTyr.[14] More recently it has been shown that replacement of the naphthyl portion of **16** by a 5-methylindolyl moiety provides a significant enhancement in Grb2 SH2 domain binding potency.[19] Using the 5-methylindolyl construct, the title pTyr mimetic Pmf was therefore examined as its N^{α}-acetyl and N^{α}-oxalyl construct (compounds **31a** and **31b**, respectively) and compared to the corresponding Pmp analogues **30a** and **30b**. As shown in Table 2, in extracellular ELISA binding assays N^{α}-acetyl **30a** (IC_{50} = 4 nM; previously reported as IC_{50} = 0.4 nM[19]) and N^{α}-oxalyl **30b** (IC_{50} = 2 nM) were substantially more potent than their corresponding naphthyl-containing homologues **24a** and **24b** (Table 1). Pmf-containing analogues **31a** and **31b** (IC_{50} = 12 nM and 8 nM, respectively) also showed potencies in the same range, although slightly reduced. In whole cell assays following extracellular administration of inhibitor, N^{α}-oxalyl **31b** was the most potent of the indolyl analogues in both inhibiting Grb2 association with phosphorylated ebrB-2 growth factor receptor (Figure 2) and in downstream MAP kinase activation (Figure 3).

Conclusions

Reported herein is the design and evaluation of a new pTyr mimetic, *p*-malonyl phenylalanine (Pmf), which in a Grb2 SH2 domain binding system is 15−20 times more potent than the previously reported *O*-malonyl tyrosine (OMT). Incorporation of Pmf into high affinity Grb2 SH2 domain-directed platforms can provide inhibitor potencies on the order of those observed using the phosphorus-containing pTyr mimetic, phosphonomethyl phenylalanine (Pmp). Both Pmp- and Pmf-containing inhibitors show potent inhibition in extracellular Grb2 binding assays, as well as in cell-based assays which measure endogenous Grb2 binding to erbB-2, MAP kinase activation. Evidence is also provided that use of an *N*-oxalyl auxiliary enhances effectiveness of inhibitors in both extracellular and intracellular contexts. Because cell membrane penetration of charged SH2 domain inhibitors has traditionally been a limiting factor in whole cell or animal assays, the favorable results in cell-based assays of Pmf-containing compounds such as **28b** may render these analogues of particular value. Such agents may have utility as potential chemotherapeutics for the treatment of various proliferative diseases, including breast cancer.

Table 2. Inhibition of Grb2 SH2 Domain Binding[a]

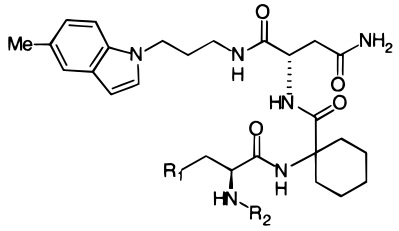

R_1	R_2 = **a** IC_{50} (μM)	R_2 = **b** IC_{50} (μM)
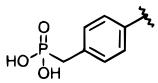 **30**	0.004 ± 0.004 (n = 4)	0.002 ± 0.008 (n = 4)
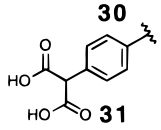 **31**	0.012 ± 0.01(n = 4)	0.008 ± 0.008(n = 4)

[a] Data were obtained using a Grb2 SH2 domain GST fusion protein in an ELISA assay as described in the Experimental Section. IC_{50} values were determined from serial dilutions of inhibitor with each concentration done in triplicate. Numbers in parentheses indicate the total number of ELISA experiments.

Experimental Section

Molecular Modeling. All simulations were performed with the Insight II 97.0/Discover 3.0 modeling package,[42] using the cff91 force field, which was modified to take into account the planarity of the oxalylamido group. A constant dielectric constant of 1.00 and the cell multipole method with fine accuracy was used for all nonbonding interactions except from the QMD simulations. The crystal structure of K-P-F-pY-V-N-V-NH_2 bound to the Grb2 SH2 domain[25] was used as the starting geometry. The structure of the heptapeptide was modified to yield **24b** within the receptor. The naphthyl ring was positioned into the hydrophobic pocket comprised by Lys 109, Leu 111, and Phe 119. All receptor and ligand atoms but the hydroxy hydrogens of Ser 88, 90, and 96, the oxalyl group, and the modified pTyr residue were held fixed during 14 quenched molecular dynamics simulations (QMD, NVT ensemble, 60 ps, different random seed for each simulation) at 800 K. The coordinates were saved every 200 fs and minimized by 300 steps of the Polak-Ribiere conjugated gradient algorithm (CG-PR). During the MD simulation the contribution of the vdw interactions was scaled to 2% and that of the Coulombic interactions to 20% in order to sample the complete conformational space. For each of the 14 runs the conformation

with the lowest energy was stored. Comparison of the resulting 14 structures showed convergence. The converged structure served as the starting geometry for 300-step CG-PR minimization followed by seven 50 ps MD (NVT-ensemble) simulations at 298 K with seven different random seed numbers, where the complex was solvated by a sphere of water with a radius of 20 Å, centered around the nitrogen of Lys 109. During minimizations and simulations, all atoms were held fixed except the ligand, the water molecules in a radius of 16 Å around the nitrogen of Lys 109, and the side chains of the Grb2 SH2 domain within 6 Å around the initial conformation of the heptapeptide of the X-ray structure. The coordinates were saved every 1 ps and minimized by 300 steps of CG-PR. The frame with lowest energy of the 350 obtained solvated structures was determined and is depicted in Figure 1a. The same QMD procedure and solvated MD simulations were repeated for **25b**, **26b**, **27b**, and **28b** (parts a, b, and c of Figure 1, respectively).

Biological. Cells and Cell Culture. Cell lines were obtained from the American Type Culture Collection (Rockville, MD) and Lombardi Cancer Center, Georgetown University Medical Center. Cells were routinely maintained in improved minimal essential medium (IMEM, Biofluids, Rockville, MD) with 10% fetal bovine serum. Cultures were maintained in a humidified incubator at 37 °C and 5% CO_2.

A. Inhibition of Grb2 SH2 Domain Binding Using ELISA Techniques. A biotinated phosphopeptide encompassing a Grb2 SH2 domain binding sequence derived from SHC protein, was bound at 20 ng/mL to 96-well plates overnight. Nonspecific interactions were inhibited by 5% bovine serum albumin containing TBS. Samples of recombinant purified Grb2 SH2-GST fusion protein were preincubated with serial dilutions of inhibitors, then added into each well. After extensive washing with 0.1% bovine serum albumin in TBS, bound Grb2 SH2 domain was detected using anti-GST antibodies and goat anti-mouse antibody conjugated to alkaline phosphatase. Quantitation of bound alkaline phosphatase was achieved by a colorimetric reaction employing *p*-nitrophenyl phosphate as substrate.

B. Inhibition of Grb2 SH2 Domain Binding in Whole Cells. ErbB2 overexpressing breast cancer cells, MDA-MB-453, were treated with inhibitors (25 μM) for 3 h in serum-free IMEM medium (Gibco). Cells were washed twice with PBS to remove inhibitor, then cell lysates were prepared using 1% Triton X-100 in PBS containing 0.2 mM $NaVO_4$. Grb2 and associated Grb2-binding proteins were immunoprecipitated from each lysate (500 μg) with anti-Grb2 antibodies and collected using protein A Sepharose. Immunoprecipitated proteins were separated by SDS−PAGE on 8−16% gradient gels (Novex), and pTyr-containing proteins were detected by Western blotting using anti-phosphotyrosine antibodies (Upstate Biochemicals Inc.). Previous experiments have shown that a major tyrosine phosphorylated protein in these cells is the p185 erbB-2, which is overexpressed as a consequence of gene amplification. Western blotting with Grb2 MAb was done as a control.

C. Inhibition of MAPK Activation in Whole Cells. The state of threonine and tyrosine phosphorylation of cellular MAP kinase (MAPK) was determined using a polyclonal antibody specifically recognizing the phosphorylated threonine and tyrosine residues of MAPK. Briefly, MDA-MB-453 cells were plated in 12-well plates and cultured in serum-free medium overnight. Cells were treated with 25 μM of various compounds for 4 h and then followed by addition of 10 nM of Heregulin stimulation. Cells were then washed twice with ice-cold PBS and lysed in 1 mL of lysis buffer (50 mM Tris-HCl, pH 7.4, 150 mM NaCl, 5 mM $MgCl_2$, 1% Triton X-100, 5 mM EDTA, 5 mM EGTA, 1 mM PMSF, 50 μg/mL approtinin, 50 μg/mL leupeptin, and 2 mM sodium orthovanadate). A protein concentration was determined by BCA method (Pierce, Rockford, IL). Protein (50 μg) was subjected to 8−20% SDS−PAGE gel (Novex, San Diego, CA) and transferred to nitrocellulose membrane. Activation of MAP kinase was detected with a specific antibody, e.g., phospho-p44/42 MAP kinase antibody (New England BioLabs) and visualized with ECL (Amersham, Arlington Heights, IL). To evaluate the equal loading of the proteins, blots were subsequently stripped and reprobed with a monoclonal antibody recognizing the total Grb2 protein or Hsp-70 protein.

Synthesis. General Synthetic Methods. Elemental analyses were obtained from Atlantic Microlab Inc., Norcross, GA, and fast atom bombardment mass spectra (FABMS) were acquired with a VG Analytical 7070E mass spectrometer under the control of a VG 2035 data system. Where indicated, FABMS matrixes used were glycerol (Gly) or nitrobenzoic acid (NBA). ^{1}H NMR data were obtained on Bruker AC250 (250 MHz) and are reported in ppm relative to TMS and referenced to the solvent in which they were run. Solvent was removed by rotary evaporation under reduced pressure, and silica gel chromatography was performed using Merck silica gel 60 with a particle size of 40−63 μm. Anhydrous solvents were obtained commercially and used without further drying. HPLCs were conducted using a Waters Prep LC4000 system having photodiode array detection and binary solvent systems as indicated where A = 0.1% aqueous TFA and B = 0.1% TFA in acetonitrile and either Vydac C_{18} (10 μm) Peptide & Protein or Advantage C_{18} (5 μ) columns (preparative size, 20 mm diameter × 250 mm long with a flow rate of 10 mL/min; semipreparative size, 10 mm diameter × 250 mm long, with a flow rate of 2 mL/min).

Benzyl (3*S*,5*S*,6*R*)-3-[4-(Bis((*tert*-butyl)oxycarbonyl)-fluoromethyl)phenylmethyl]-(−)-6-oxo-5,6-diphenyl-4-morpholine-carboxylate (13). To the suspension of 60% NaH in oil (150 mg, 3.75 mmol) in anhydrous THF (30 mL) was added a solution of benzyl (3*S*,5*S*,6*R*)-3-[4-(bis((*tert*-butyl)-oxycarbonyl)methyl)phenylmethyl]-(−)-6-oxo-5,6-diphenyl-4-morpholine-carboxylate[36] (2.075 g, 3.0 mmol) in anhydrous THF (30 mL) at 0 °C, and then the resulting mixture was stirred at room temperature (1 h). The solution was cooled to 0 °C, and benzenesulfonamino fluoride (950 mg, 3.0 mmol) in anhydrous THF (20 mL) was added dropwise. The reaction mixture was stirred (0 °C, 2.5 h), then quenched with saturated aqueous ammonium chloride (50 mL), subjected to an extractive workup (EtOAc), dried (Na_2SO_4), and taken to dryness. Purification by silica gel flash chromatography (EtOAc−hexanes, from 1:10 to 1:6) provided **13** as a white solid (1.96 g, 92%): ^{1}H NMR ($CDCl_3$; two conformers were observed in a ratio of 4:9 at 23 °C) major conformer δ 7.60 (2H, d, J = 8.1 Hz), 7.41∼7.00 (12 H, m), 6.81 (1H, d, J = 7.3), 6.56 (2H, m), 6.48 (2H, d, J = 7.3 Hz), 5.35 (1H, dd, J = 2.4, 6.10 Hz, -OOCCH-N), 5.08 (1H, d, J = 12.2 Hz, OCH_2Ph), 4.99 (1H, d, J = 12.7 Hz, OCH_2Ph), 4.80 (1H, d, J = 2.93 Hz, -PhCHOOC), 4.15 (1H, d, J = 2.93 Hz, -PhCHN-), 3.57 (1H, dd, J = 6.4, 13.7 Hz, -CH_2-CHNCOO), 3.42 (1H, dd, J = 2.4, 13.4 Hz, -CH_2-CHNCOO), 1.52 (9H, s), 1.41 (9H, s), minor confomer δ 7.54 (2H, d, J = 8.1 Hz), 7.41∼7.00 (13 H, m, overlapping), 6.56∼6.64 (4H, m, overlapping), 5.32 (1H, d, J = 12.2 Hz, OCH_2Ph), 5.26 (1H, dd, J = 2.9, 6.4 Hz, -OOCCH-N), 5.11 (1H, d, J = 12.0 Hz, OCH_2Ph), 4.97 (1H, overlapping, -PhCHOOC), 4.36 (1H, d, J = 2.7 Hz, -PhCHN-), 3.57 (1H, dd, J = 6.8, 13.7 Hz, -CH_2-CHNCOO), 3.37 (1H, dd, J = 2.9, 13.7 Hz, -CH_2-CHNCOO), 1.52 (9H, s, overlapping), 1.43 (9H, s); FABMS (+VE, NBA) *m/z* 598.8 [$MH^+ - 2\ C_4H_8$], 554.8 [$MH^+ - 2C_4H_8 - CO_2$], 510.7 [$MH^+ - 2C_4H_8 - 2CO_2$]. Anal. ($C_{42}H_{44}FNO_8$) C, H, N.

***N*$^\alpha$-Fmoc-4-(bis((*tert*-butyl)oxycarbonyl)fluoromethyl)-L-phenylalanine (15).** A solution of **13** (1.76 g, 2.49 mmol) in THF−EtOH (1:1, 20 mL), with 2 drops of AcOH added to promote reaction, was hydrogenated over 150 mg of Pd black (45 psi H_2, room temperature, 5 h). Catalyst was removed by filtration, and combined organics were concentrated to give crude free amino acid **14** as a white sticky solid. A mixture of crude **14**, Fmoc-OSu (881 mg, 2.49 mmol), and Na_2CO_3 (791 mg, 74.5 mmol) in 35 mL of dioxane−water (1:1) was stirred at room temperature (overnight), then cooled to 0 °C, acidified with 0.2 M HCl (120 mL), and subjected to an extractive

workup (EtOAc). Removal of solvent and purification by silica gel chromatography ($CHCl_3$−EtOAc−MeOH) to provided product **15** as a white solid (1.28 g, 85% from **13**): ^{1}H NMR (DMSO) δ 12.70 (1H, br s), 7.87 (2H, d, J = 7.3 Hz), 7.79 (1H, d, J = 8.6 Hz), 7.65 (2H, t, J = 7.3 Hz), 7.44∼7.23 (8H, m), 4.22∼4.10 (4H, m), 3.12 (1H, dd, J = 3.7, 13.4 Hz), 2.90 (1H, dd, J = 10.7, 13.7 Hz), 1.42 (9H, s), 1.42 (9H, s); FABMS (+VE, NBA) m/z 618 [M − H]. HR-FABMS calcd for $C_{35}H_{37}FNO_8$ (M − H) m/z, 618.2503; found, 618.2484.

Determination of Enantiomeric Purity of 15. Enantiomeric purity of **15** was determined using previously reported procedures.[34] L-Leu-Rink amide resin (12.5 mg, 5 μmol based on 0.4 mmol/g; Bachem Corp., Torrance, CA) was washed well with several 1 mL portions of *N*-methyl-2-pyrrolidinone (NMP), and Fmoc amino protection was removed by treatment with 20% piperidine in NMP (0.5 mL, 1 min; then 0.5 mL, 20 min). The deblocked resin was washed well with NMP (10 × 1 mL), then coupled overnight with a solution of active ester formed by reacting **15** (12.5 μmol), 1-hydroxybenzotriazole (HOBt), and 1,3-diisopropyl-carbodiimide (DIPCDI) in NMP (1.0 mL, 10 min). The resin was washed with NMP (10 × 1 mL), and the N-terminal Fmoc protection was removed by treatment with 20% piperidine in NMP (0.5 mL, 5 min). The deblocked resin was washed with NMP (10 × 1 mL) and dichloromethane (10 × 2 mL), then dipeptide was cleaved using a mixture of TFA (1.85 mL), H_2O (100 mL), and triethylsilane (50 μL) (1 h), and the resulting dipeptide was analyzed using a semi-preparative Vydac column with linear gradient from 5% B to 30% B over 25 min). An identical procedure repeated using d,L-Leu-Rink amide resin, provided a reference mixture of diastereomeric D,L-leucine dipeptides, which gave HPLC retention times for diastereomeric peaks at 16.61 min and 20.64 min. On this basis, diastereomeric contamination in the L-leucine dipeptide accounted for area less than 3% of that observed for the major diastereomer, indicating that greater than 97% of a single enantiomer was present in **15**.

General Procedure for the Synthesis of Compounds 17a−19a. To the solution of **16**[1] (46 mg, 0.1 mmol) in anhydrous DMF (2 mL) was added an active ester solution formed by reacting N^{α}-Fmoc/*O*-(*tert*-butyl)-protected pTyr mimetics OMT,[31] Pmf,[36] or **15** (0.1 mmol), HOBt·H_2O (14 mg, 0.1 mmol), and DIPCDI (16 μL, 0.1 mmol) in anhydrous DMF (2 mL) at room temperature (10 min). The resulting reaction mixtures were stirred at room temperature (overnight), then solvent was removed under high vacuum, and residues were purified by silica gel chromatography ($CHCl_3$:EtOAc:MeOH) to provide products as white foams.

Compound 17a (68% yield): ^{1}H NMR ($CDCl_3$) δ 8.14∼8.02 (2H, m), 7.92∼7.64 (6H, m), 7.58∼7.30 (9H, m), 7.08 (2H, d, J = 8.1 Hz), 6.91 (2H, d, J = 8.1 Hz), 6.88 (1H, brs), 6.43 (1H, brs), 5.59 (1H, brs), 5.43 (1H, d, J = 6.8 Hz), 5.01 (1H, s), 4.83∼4.70 (1H, m), 4.25∼4.16 (2H, m), 3.48∼3.32 2H, m), 3.18∼2.85 (5H, m), 2.64 (1H, dd, J = 8.1,15.4 Hz), 2.15∼1.15 (12H, m), 1.58 (18H, s); FABMS (+VE, NBA) m/z 1024.9 [MH^+].

Compound 18a (100% yield): ^{1}H NMR ($CDCl_3$) δ 8.01 (2H, m), 7.81∼7.71 (6H, m), 7.50∼6.95 (13H, m), 6.58 (1H, s), 5.56 (3H, m), 4.69 (1H, m), 4.55∼4.40 (1H, m), 4.40 (1H, s), 4.31 (2H, d, J = 6.84 Hz), 4.09 (1H, m), 3.34 (1H, m), 3.12∼2.88 (5 H, m), 2.63 (1H, dd, J = 4.4, 15.1 Hz), 2.05∼1.11 (12H, m), 1.46 (18H, s); FABMS (+VE, NBA) m/z 1008 [MH^+].

Compound 19a (97% yield): ^{1}H NMR ($CDCl_3$) δ 8.30∼8.14 (1H, s, br), 8.07∼8.00 (2H, m), 7.83∼7.64 (5H, m), 7.55∼7.10 (14H, m), 6.85∼6.76 (1H, s, br), 5.70∼5.60 (1H, s, br), 5.40 (1H, m), 4.68 (1H, m), 4.55∼4.30 (3H, m), 4.14 (1H, t, J = 6.6 Hz), 3.38 (2H, m), 3.15∼2.62 (6H, m), 2.10∼1.00 (12H, m), 1.50 (18H, s); FABMS (+VE, NBA) m/z 1026 [MH^+].

General Procedure for the Synthesis of Compounds 17c−19c. To solutions of tripeptides **17a−19a** (0.05 mmol) in anhydrous acetonitrile (2 mL) was added piperidine (40 μL, 0.4 mmol), and the solutions were stirred at room temperature (3 h). Solvent and excess piperidine were removed under high vacuum, and crude free amines **17b−19b** were dissolved in anhydrous acetonitrile or DMF (3 mL) and treated overnight with *N*-acetylimidazole (55 mg, 0.5 mmol). Solvent was removed, and residues were purified by silica gel chromatography ($CHCl_3$−EtOAc−MeOH) to provide products as white foams.

Compound 17c (99%): ^{1}H NMR ($CDCl_3$) δ 8.28∼8.02 (2H, m), 7.90∼7.45 (3H, m), 7.90∼7.45 (3H, m), 7.64∼7.34 (4H, m), 7.10 (2H, d, J = 8.6 Hz), 6.89 (2H, d, J = 8.6 Hz), 6.57 (1H, brd, J = 6.8 Hz), 6.49 (1H, brs), 5.76 (1H, brs), 5.02 (1H, s), 4.84∼4.72 (1H, m), 4.68∼4.58 (1H, m), 3.48∼3.36 (2H, m), 3.20∼2.84 (5H, m), 2.65 (1H, dd, J = 8, 15 Hz), 2.15∼1.15 (12H, m), 1.58 (18H, s); FABMS (+VE, NBA) m/z 844 [MH^+].

Compound 18c (94% yield): ^{1}H NMR ($CDCl_3$) δ 8.03 (2H, m), 7.81 (1H, m), 7.63 (3H, m), 7.46∼7.05 (9H, m), 6.65 (2H, m), 4.67 (2H, m), 4.40 (1H, s), 3.34 (2H, m), 3.12∼2.89 (5 H, m), 2.55 (1H, dd, J = 4.60, 15.1 Hz), 1.81 (3H, s), 2.04∼1.15 (12H, m), 1.46 (18H, s); FABMS (+VE, NBA) m/z 828 [MH^+], 772 [$MH^+ - C_4H_8$].

Compound 19c (94% yield): ^{1}H NMR ($CDCl_3$) δ 8.05 (2H, m), 7.80 (1H, m), 7.66 (2H, m), 7.55∼7.05 (9H, m), 6.62 (1H, brs), 6.37 (1H, d, J = 6.10 Hz), 5.83 (1H, s), 4.69 (2H, m), 3.34 (2H, m), 3.15∼2.85 (5H, m), 2.55 (1H, dd, J = 4.15, 15.14 Hz), 2.10∼0.83 (12H, m), 1.81 (3H, s), 1.50 (18H, s); FABMS (+VE, NBA) m/z 846 [MH^+].

General Procedure for the Synthesis of Compounds 17d−19d. To solutions of tripeptides **17a−19a** (0.05 mmol) in anhydrous acetonitrile (2 mL) was added piperidine (40 μL, 0.4 mmol), and the solutions were stirred at room temperature (3 h). Solvent and excess piperidine were removed under high vacuum, crude free amines **17b−19b** were dissolved in anhydrous DMF (2 mL), and diisopropyl ethylamine (22 μL, 0.125 mmol) was added followed by *tert*-butyl oxalyl chloride (16 μL, 0.125 mmol). The reaction mixtures were stirred at room temperature (overnight), and then the mixtures were concentrated and purified by silica gel chromatography ($CHCl_3$−EtOAc−MeOH) to provide products as white foams.

Compound 17d (94%): ^{1}H NMR ($CDCl_3$) δ 8.18∼8.09 (1H, m), 8.04 (1H, d, J = 8.1 Hz), 7.95∼7.90 (1H, m), 7.85∼7.66 (2H, m), 7.60∼7.48 (2H, m), 7.44 (2H, d, J = 4.7 Hz), 7.23 (2H, d, J = 8.5 Hz), 6.95 (2H, d, J = 8.5 Hz), 6.49 (1H, brs), 6.17 (1H, brs), 5.59 (1H, brs), 5.02 (1H, s), 4.84∼4.72 (1H, m), 4.68∼4.58 (1H, m), 3.48∼3.36 (2H, m), 3.25∼2.96 (5H, m), 2.58 (1H, dd, J = 5.1, 15.0 Hz), 2.05∼0.97 (12H, m), 2.15∼1.15 (18H, s), 1.56 (9H, s); FABMS (+VE, NBA) m/z 930.6 [MH^+].

Compound 18d (50% yield): ^{1}H NMR ($CDCl_3$) δ 8.02 (2H, m), 7.83∼7.21 (13H, m), 6.69 (1H, s), 6.38 (1H, s), 4.67 (2H, m), 4.40 (1H, s), 3.43∼2.88 (7 H, m), 2.56 (1H, dd, J = 4.9, 14.9 Hz), 2.05∼0.94 (12H, m), 1.46 (18H, s), 1.46 (9H, s); FABMS (+VE, NBA) m/z 914 [MH^+].

Compound 19d (90% yield): ^{1}H NMR ($CDCl_3$) δ 8.06 (2H, m), 7.85∼7.24 (12H, m), 6.80 (1H, s), 6.57 (1H, s), 5.66 (1H, s), 4.75∼4.60 (2H, m), 3.34 (2H, m), 3.18∼2.95 (5H, m), 2.53 (1H, dd, J = 4.6, 14.9 Hz), 2.05∼0.97 (12H, m), 1.50 (18H, s), 1.47 (9H, s); FABMS (+VE, NBA) m/z 932.8 [MH^+].

General Procedure for the Conversion of Protected Derivatives 17c−19c and 17d−19d to Final Products 25a, 28a, 29a and 25b, 28b, 29b, Respectively. Protected analogues **17c−19c** and **17d−19d** (0.05∼0.1 mmol) were treated (1 h) with solutions of TFA (1.90 mL):H_2O (0.10 mL):triethylsilane (0.05 mL), taken to dryness, and purified by HPLC to yield products as white solids.

Compound 25a. Purification by preparative HPLC (Advantage column; linear gradient from 10% B to 90% B over 20 min; retention time, 15.6 min) yielded product as a white powder (62% yield): ^{1}H NMR (DMSO-d_6) δ 8.28∼8.21 (2H, brs), 8.17∼8.10 (1H, m), 8.04∼7.92 (2H, m), 7.79 (1H, t, J = 4.2 Hz), 7.58∼7.50 (2H, m), 7.46∼7.38 (2H, m), 7.20 (2H, d, J = 8.6 Hz), 6.93 (1H, brs), 6.87 (2H, d, J = 8.6 Hz), 5.34 (1H, s), 4.96∼4.58 (1H, m), 4.45∼4.35 (1H, m), 3.28∼2.98 (5H, m), 2.85∼2.60 (2H, m), 2.05∼1.10 (12H, m), 1.80 (3H, s); semi-preparative HPLC retention time: 21.6 min (Vydac column; linear gradient from 10% B to 90% B over 20 min); FABMS (−VE, Gly), m/z 730 [M − H]. HR-FABMS calcd for $C_{37}H_{44}FN_5O_8$ [M − H − CO_2] m/z, 686.3190; found, 686.3182.

Compound 28a. Purification by preparative HPLC (Advantage column; linear gradient from 5% B to 50% B over 15 min; retention time, 19.2 min) yielded product as a white powder (73% yield): ^{1}H NMR (DMSO-d_6) δ 8.25 (2H, m), 8.08 (1H, m), 7.99 (1H, m), 7.90 (1H, m), 7.74 (1H, m), 7.51∼7.18 (10H, m), 6.90 (1H, s), 4.65 (1H, m), 4.60 (1H, s), 4.36 (1H, m), 3.35∼2.98 (5H, m), 2.82∼2.56 (3H, m), 1.78 (3H, s), 2.08∼1.12 (12H, m); semipreparative HPLC retention time: 25.19 min (Vydac column; linear gradient from 0% B to 50% B over 15 min, then from 50% B to 60% B over 15 min); FABMS (−VE, Gly) *m*/*z* 714 [M − H], 670 [M − H − CO_2], 626 [M − H − 2CO_2]. HR-FABMS calcd for $C_{38}H_{45}N_5O_9$ [M − H] *m*/*z*, 714.3139; found, 714.3199.

Compound 29a. Purification by preparative HPLC (Advantage column; linear gradient from 10% B to 90% B over 20 min; retention time, 15.4 min) yielded product as a white powder (86% yield): ^{1}H NMR (DMSO-d_6) δ 8.30∼8.20 (2H, m), 8.08 (1H, m), 7.99 (1H, d, J = 8.1 Hz), 7.88 (1H, m), 7.74 (1H, t, J = 4.9 Hz), 7.55∼7.22 (10H, m), 6.90 (1H, s), 4.65 (1H, m), 4.35 (1H, m), 3.30∼2.55 (8H, m), 1.77 (3H, s), 2.00∼1.00 (12H, m); semipreparative HPLC retention time: 22.78 min (Vydac column; linear gradient from 0% B to 90% B over 25 min); FABMS (−VE, Gly) *m*/*z* 732.9 [M − H], 688.9 [M − H − CO_2], 644.9 [M − H − 2CO_2]. HR-FABMS calcd for $C_{37}H_{43}FN_5O_7$ [M − H − CO_2] *m*/*z*, 688.3147; found, 688.3121.

Compound 25b. Purification by preparative HPLC (Advantage column; linear gradient from 10% B to 90% B over 20 min; retention time, 15.6 min) yielded product as a white powder (71% yield): ^{1}H NMR (DMSO-d_6) δ 8.82 (1H, d, J = 7.7 Hz), 8.35 (1H, brs), 8.18∼8.10 (1H, m), 8.04 (1H, d, J = 8.1 Hz), 7.97∼7.92 (1H, m), 7.79 (1H, t, J = 4.7 Hz), 7.60∼7.52 (2H, m), 7.46∼7.40 (2H, m), 7.22 (2H, d, J = 8.1 Hz), 6.96 (1H, brs), 6.86 (2H, d, J = 8.1 Hz), 5.35 (1H, s), 4.74∼4.70 (1H, m), 4.48∼4.35 (1H, m), 3.23∼2.65 (7H, m), 2.10∼1.10 (12H, m); semipreparative HPLC retention time: 15.1 min (Vydac column; linear gradient from 10% B to 90% B over 20 min); FABMS (−VE, Gly) *m*/*z* 760 [M − H]. HR-FABMS calcd for $C_{37}H_{42}FN_5O_{10}$ [M − H − CO_2] *m*/*z*, 716.2932; found, 716.2879.

Compound 28b. Purification by preparative HPLC (Advantage column; linear gradient from 5% B to 50% B over 15 min; retention time, 18.5 min) yielded product as a white powder (52% yield): ^{1}H NMR (DMSO-d_6) δ 8.82 (1H, s), 8.08 (1H, m), 8.00 (1H, d, J = 7.3 Hz), 7.89 (1H, m), 7.74 (1H, m), 7.53∼7.20 (10H, m), 6.92 (1H, s), 4.73 (1H, m), 4.60 (1H, s), 4.36 (1H, m), 3.25∼2.93 (6H, m), 2.69 (1H, dd, J = 6.8, 15.4 Hz), 2.52 (1H, m), 2.08∼1.12 (12H, m); semipreparative HPLC retention time: 24.35 min (Vydac column; linear gradient from 0% B to 50% B over 15 min, then from 50% B to 60% B over 15 min); FABMS (−VE, Gly) *m*/*z* 744 [M − H], 700 [M − H − CO_2]. HR-FABMS calcd for $C_{37}H_{42}N_5O_9$ [M − H − CO_2] *m*/*z*, 700.2983; found, 700.2966.

Compound 29b. Purification by preparative HPLC (Advantage column; linear gradient from 10% B to 90% B over 20 min; retention time, 14.9 min) yielded product as a white powder (63% yield): ^{1}H NMR (DMSO-d_6) δ 8.85 (1H, d, J = 7.8 Hz), 8.32 (1H, s), 8.08 (1H, m), 7.99 (1H, d, J = 8.1 Hz), 7.88 (1H, m), 7.83 (1H, t, J = 4.9 Hz), 7.55∼7.22 (10H, m), 6.91 (1H, s), 4.37 (1H, m), 4.30 (1H, m), 3.25∼2.91 (7H, m), 2.68 (1H, dd, J = 6.4, 15.4 Hz), 2.06∼0.93 (12H, m); semipreparative HPLC retention time: 22.05 min (Vydac column; linear gradient from 0% B to 90% B over 25 min); FABMS (−VE, Gly) *m*/*z* 762 [M − H], 718 [M − H − CO_2]. HR-FABMS calcd for $C_{37}H_{41}FN_5O_9$ [M − H − CO_2] *m*/*z*, 718.2888; found, 718.2849.

Synthesis of Dipeptide 21a. A mixture of N^{α}-Fmoc 1-aminocyclohexanylcarboxylic acid (2.85 g, 7.80 mmol), HOBt·H_2O (1.19 g, 5.80 mmol) and DIPCDI (1.22 mL, 7.80 mmol) in DMF (40 mL) was stirred at room temperature (1 h), then freshly prepared 3-(*N*-(5-methylindolyl))propanamido-L-asparagine (**20**)[19] (7.80 mmol) in DMF (10 mL) was added, and the reaction mixture was stirred at room temperature (overnight). The mixture was poured into ice−water (200 mL) and subjected to an extractive workup (EtOAc). Silica gel chromatographic purification of the concentrated residue ($CHCl_3$−EtOAC, 10:1 to $CHCl_3$−MeOH, 20:1) provided **21a** as a light-yellow solid (4.89 g, 96%): ^{1}H NMR (DMSO-d_6) δ 8.08 (1H, d, J = 7.3 Hz), 7.89 (2H, d, J = 7.6 Hz), 7.78 (1H, s), 7.65 (2H, dd, J = 8.0, 9.6 Hz), 7.50∼7.20 (9H, m), 6.92 (1H, s), 6.85 (1H, d, J = 8.3 Hz), 6.21 (1H, d, J = 2.7 Hz), 4.38 (1H, m), 4.30∼4.15 (3H, m), 4.05 (2H, m), 2.96 (2H, m), 2.64 (1H, dd, J = 15.1, 6.6 Hz), 2.54∼2.46 (1H, dd, partially covered by DMSO peaks), 2.33 (3H, s), 1.98∼1.20 (12H, brm); FABMS (+VE, NBA) *m*/*z* 650 [MH$^+$].

General Procedure for the Synthesis of Compounds 22a−23a. Synthesis of tripeptides **22a** and **23a** were accomplished by coupling free amine **21b** (obtained by reacting **21a** with piperidine in DMF followed by removal of solvent under high vacuum) with appropriately protected amino acids in fashions similar to that described above for the synthesis of **17a** and **17b**, respectively.

Compound 22a (52% yield): ^{1}H NMR ($CDCl_3$) δ 8.37 (1H, s), 8.32 (1H, s), 8.10∼7.90 (4H, m), 7.80∼7.65 (2H, m), 7.60∼6.90 (14H, m), 6.36∼6.30 (1H, m), 4.57∼4.35 (2H, m), 4.23∼4.10 (4H, m), 3.38 (1H, s), 3.35 (1H, s), 3.16∼2.60 (4H, m), 2.39 (3H, s), 2.10∼0.84 (12H, m), 1.38 (18H, s); FABMS (+VE, NBA) *m*/*z* 1003.7 (MH$^+$).

Compound 23a (quantitative): ^{1}H NMR ($CDCl_3$) δ 8.06∼6.94 (21H, m), 6.56 (1H, s), 6.32 (1H, d, J = 2.7 Hz), 4.62 (1H, m), 4.46 (1H, m), 4.40 (1H, s), 4.34 (2H, d, J = 6.8 Hz), 4.12 (3H, m), 3.30∼2.80 (5H, m), 2.64 (1H, dd, J = 3.4, 14.65 Hz), 2.40 (3H, s), 2.10∼0.84 (12H, m), 1.45 (18H, s); FABMS (+VE, NBA) *m*/*z* 1011.6 [MH$^+$], 955.6 [MH$^+$ − C_4H_8].

General Procedure for the Synthesis of Compounds 22c and 23c. Synthesis of acetylated tripeptides **22c** and **23c** were accomplished by piperidine treatment of N^{α}-Fmoc protected **22a** and **23a** followed by acetylation with *N*-acetylimidazole and chromatographic purification similar to that described above for the conversion of **17a** and **18a** to **17c** and **18c**, respectively.

Compound 22c (quantitative): ^{1}H NMR (DMSO-d_6) δ 8.30 (1H, s), 8.26 (1H, d, J = 7.3 Hz), 8.04∼7.96 (1H, m), 7.72 (1H, brs), 7.55∼6.90 (10H, m), 6.33 (1H, d, J = 1.6 Hz), 4.75∼4.62 (1H, m), 4.43∼4.32 (1H, m), 4.18 (2H, t, J = 6.8 Hz), 3.15∼2.60 (6H, m), 2.40 (3H, s), 2.06∼1.15 (12H, m), 1.79 (3H, s), 1.40 (18H, s); FABMS (+VE, NBA) *m*/*z* 823 [MH$^+$].

Compound 23c (quantitative): ^{1}H NMR ($CDCl_3$) δ 8.08 (1H, d, J = 7.8 Hz), 7.66 (2H, m), 7.36∼6.94 (10 H, m), 6.32 (1H, d, J = 2.9 Hz), 6.03 (1H, s), 4.70∼4.55 (2H, m), 4.41 (1H, s), 4.11 (2H, t, J = 6.6 Hz), 3.25∼3.05 (3H, m), 3.00∼2.85 (2H, m), 2.65 (1H, dd, J = 4.4 Hz), 2.40 (3H, s), 2.10∼1.05 (12H, m), 1.86 (3H, s), 1.46 (18H, s); FABMS (+VE, NBA) *m*/*z* 831 [MH$^+$], 775 [MH$^+$ − C_4H_8].

General Procedure for the Synthesis of Compounds 22d and 23d. Synthesis of tripeptides **22d** and **23d** were accomplished by piperidine treatment of N^{α}-Fmoc protected **22a** and **23a** followed by acylation with *tert*-butyl oxalyl chloride and chromatographic purification similar to that described above for the conversion of **17a** and **18a** to **17d** and **18d**, respectively.

Compound 22d (quantitative): ^{1}H NMR (DMSO-d_6) δ 8.78 (1H, d, J = 4.7 Hz), 8.44∼8.31 (2H, m), 8.07∼7.96 (2H, m), 7.66∼7.16 (7H, m), 6.95 (2H, d, J = 9.0 Hz), 6.33 (1H, d, J = 3.8 Hz), 4.80∼4.66 (1H, m), 4.46∼4.34 (1H, m), 4.18 (1H, t, J = 6.4 Hz), 3.25∼2.60 (6H, m), 2.40 (3H, s), 2.10∼1.05 (12H, m), 1.48 (9H, s), 1.37 (18H, s); FABMS (+VE, NBA) *m*/*z* 909 [MH$^+$].

Compound 23d (94% yield): ^{1}H NMR ($CDCl_3$) δ 7.96 (1H, d, J = 7.8 Hz), 7.68 (1H, d, J = 7.1 Hz), 7.50 (1H, m), 7.38∼7.24 (8H, m), 7.18 (1H, d, J = 2.9 Hz), 7.00 (1H, d, J = 8.3 Hz), 6.36 (1H, d, J = 2.9 Hz), 6.03 (1H, s, br), 4.66 (2H, m), 4.41 (1H, s), 4.17 (2H, t, J = 6.8 Hz), 3.26 (2H, m), 3.12 (2H, d, J = 7.3 Hz), 3.08∼3.00 (1H, dd, J = 4.6, 15.1 Hz), 2.58∼2.50 (1H, dd, J = 4.9, 15.14 Hz), 2.43 (3H, s), 2.10∼1.00 (12H, m), 1.51 (9H, s), 1.47 (18H, s); FABMS (+VE, NBA) *m*/*z* 917 [MH$^+$], 861 [MH$^+$ − C_4H_8].

General Procedure for the Conversion of Protected Derivatives 22c, 23c and 22d, 23d to Final Products 30a,

31a and 30b, 31b, Respectively. Protected analogues **22c**, **23c** and **22d**, **23d** (~0.1 mmol) were treated (1 h) with solutions of TFA (1.90 mL):H_2O (0.10 mL):1,2-ethanedithiol (0.05 mL), taken to near dryness, and triturated with anhydrous ether to yield solids which were suspended in ether, collected, and dried to provide crude **30a**, **31a** and **30b**, **31b**, respectively, as white or slightly pink solids. Final products were obtained by HPLC purification.

Compound 30a. Purification by preparative HPLC (Advantage column; linear gradient from 30% B to 90% B over 20 min; retention time, 11.5 and 12.1 min) yielded product as a white powder (27% yield): ^{1}H NMR (D_2O) δ 8.08 (1H, brs), 7.56~7.38 (3H, m), 7.33~7.05 (6H, m), 5.75~5.60 (1H, m), 4.70~4.55 (1H, m), 4.53~4.40 (1H, m), 4.33~4.20 (2H, m), 3.90~2.70 (6H, m), 2.55 (1.5H, s), 2.45 (1.5H, s), 2.20~1.0 (15H, m); semipreparative HPLC retention time: 8.4 and 10.4 min (Vydac column; linear gradient from 40% B to 90% B over 20 min) [Note: compound exists as two interconverting forms on HPLC]; FABMS (−VE, Gly) *m*/*z* 709.2 (M − H). HR-FABMS calcd for $C_{35}H_{46}N_6O_8P$ [M − H] *m*/*z*, 709.3115; found, 709.3091.

Compound 30b. Purification by preparative HPLC (Advantage column; linear gradient from 10% B to 90% B over 20 min; retention time, 15.3 and 15.7 min) yielded product as a white powder (67% yield): ^{1}H NMR (D_2O) δ 8.28~8.20 (1H, m), 7.58~7.05 (9H, m), 5.75~5.60 (1H, m), 4.70~4.45 (1H, m), 4.30~4.14 (1H, m), 3.90~2.70 (6H, m), 2.55~2.40 (3H, m), 2.25~1.12 (12H, m); semipreparative HPLC retention time: 19.0 and 21.0 min (Vydac column; linear gradient from 10% B to 90% B over 20 min) [Note: compound exists as two interconverting forms on HPLC]; FABMS (−VE, Gly) *m*/*z* 739.2 (M − H). HR-FABMS calcd for $C_{35}H_{44}N_6O_{10}P$ [M − H] *m*/*z*, 739.2857; found, 739.2881.

Compound 31a. Purification by preparative HPLC (Vydac column; linear gradient from 10% B to 90% B over 20 min; retention time, 16.0 min) yielded product as a light pink powder (54% yield): ^{1}H NMR (DMSO) δ 8.30~8.20 (2H, m), 7.97 (1H, d, J = 7.6 Hz), 7.45~7.15 (9H, m), 6.95~6.75 (2H, m), 6.28 (1H, d, J = 2.9 Hz), 4.70~4.60 (1H, m), 4.60 (1H, s), 4.30 (1H, m), 4.13 (2H, t, J = 6.6 Hz), 3.10~2.57 (6H, m), 2.35 (3H, s), 2.00~1.00 (12H, m), 1.79 (3H, s); semipreparative HPLC retention time: 26.20 min (Vydac column; linear gradient from 10% B to 90% B over 30 min); FABMS (−VE, Gly) *m*/*z* 717 [M − H], 673 [M − H − CO_2]. HR-FABMS calcd for $C_{37}H_{46}N_6O_9$ [M − H] *m*/*z*, 717.3248; found, 717.3221.

Compound 31b. Purification by preparative HPLC (Vydac column; linear gradient from 10% B to 90% B over 20 min; retention time, 15.4 min) yielded product as a light pink powder (47% yield): ^{1}H NMR (DMSO) δ 8.90~8.75 (1H, m), 8.29 (1H, m), 8.00~7.85 (1H, m), 7.50~7.07 (9H, m), 7.00~6.69 (3H, m), 4.71 (1H, m), 4.49 (1H, s), 4.32 (1H, m), 4.15~4.04 (2H, m), 3.25~2 0.55 (6H, m), 2.35~2.17 (3H, several single peaks), 2.00~1.11 (12H, m); semipreparative HPLC retention time: 24.67 min (Vydac column; linear gradient from 10% B to 90% B over 30 min); FABMS (−VE, Gly) *m*/*z* 747 [M − H], 703 [M − H − CO_2]. HR-FABMS calcd for $C_{36}H_{43}N_6O_9$ [M − H − CO_2] *m*/*z*, 703.3092; found, 703.3092.

References

(1) Yao, Z. J.; King, C. R.; Cao, T.; Kelley, J.; Milne, G. W. A.; Voigt, J. H.; Burke, T. R. Potent inhibition of Grb2 SH2 domain binding by nonphosphate-containing ligands. *J. Med. Chem.* **1999**, *42*, 25−35.

(2) Yao, Z.-J.; Luo, J. H.; Gao, Y.; Yang, D.; Voigt, J.; King, C. R.; Burke, T. R., Jr. Synthesis and evaluation of high affinity nonphosphate containing Grb2 SH2 domain ligands. *Abstracts of Papers*, 217th National Meeting of the American Chemical Society, Anaheim, CA, March 21−25, 1999; American Chemical Society: Washington, DC, 1999; MEDI 176.

(3) Ponzetto, C. Physiological function of receptor-SH2 interactions. *Protein Modules in Signal Transduction* **1998**, *228*, 165−177.

(4) Dankort, D. L.; Wang, Z. X.; Blackmore, V.; Moran, M. F.; Muller, W. J. Distinct tyrosine autophosphorylation sites negatively and positively modulate neu-mediated transformation. *Mol. Cell. Biol.* **1997**, *17*, 5410−5425.

(5) Rojas, M.; Yao, S. Y.; Lin, Y. Z. Controlling epidermal growth factor (EGF)-stimulated ras activation in intact cells by a cell-permeable peptide mimicking phosphorylated EGF receptor. *J. Biol. Chem.* **1996**, *271*, 27456−27461.

(6) Williams, E. J.; Dunican, D. J.; Green, P. J.; Howell, F. V.; Derossi, D.; Walsh, F. S.; Doherty, P. Selective inhibition of growth factor-stimulated mitogenesis by a cell-permeable Grb2-binding peptide. *J. Biol. Chem.* **1997**, *272*, 22349−22354.

(7) Burke, T. R., Jr.; Smyth, M. S.; Otaka, A.; Nomizu, M.; Roller, P. P.; Wolf, G.; Case, R.; Shoelson, S. E. Nonhydrolyzable phosphotyrosyl mimetics for the preparation of phosphatase-resistant SH2 domain inhibitors. *Biochemistry* **1994**, *33*, 6490−6494.

(8) Ye, B.; Akamatsu, M.; Shoelson, S. E.; Wolf, G.; Giorgetti-Peraldi, S.; Yan, X. J.; Roller, P. P.; Burke, T. R. L-O-(2-malonyl)-tyrosine: A new phosphotyrosyl mimetic for the preparation of Src homology 2 domain inhibitory peptides. *J. Med. Chem.* **1995**, *38*, 4270−4275.

(9) Gay, B.; Furet, P.; Garcia-Echeverria, C.; Rahuel, J.; Chene, P.; Fretz, H. Dual specificity of Src homology 2 domains for phosphotyrosine peptide ligands. *Biochemistry* **1997**, *36*, 5712−5718.

(10) Furet, P.; Gay, B.; Garcia-Echeverria, C.; Rahuel, J.; Fretz, H.; Schoepfer, J.; Caravatti, G. Discovery of 3-aminobenzyloxycarbonyl as an N-terminal group conferring high affinity to the minimal phosphopeptide sequence recognized by the Grb2-SH2 domain. *J. Med. Chem.* **1997**, *40*, 3551−3556.

(11) Oligino, L.; Lung, F. D. T.; Sastry, L.; Bigelow, J.; Cao, T.; Curran, M.; Burke, T. R.; Wang, S. M.; Krag, D.; Roller, P. P.; King, C. R. Nonphosphorylated peptide ligands for the Grb2 Src homology 2 domain. *J. Biol. Chem.* **1997**, *272*, 29046−29052.

(12) Schoepfer, J.; Gay, B.; Caravatti, G.; Garcia-Echeverria, C.; Fretz, H.; Rahuel, J.; Furet, P. Structure-based design of peptidomimetic ligands of the Grb2-SH2 domain. *Bioorg. Med. Chem. Lett.* **1998**, *8*, 2865−2870.

(13) Garcia-Echeverria, C.; Furet, P.; Gay, B.; Fretz, H.; Rahuel, P.; Schoepfer, J.; Caravatti, G. Potent antagonists of the SH2 domain of Grb2: Optimization of teh X=1 position of 3-amino-Z-Tyr(PO3H2)-X+1-Asn-NH2. *J. Med. Chem.* **1998**, *41*, 1741−1744.

(14) Furet, P.; Gay, B.; Caravatti, G.; Garcia-Echeverria, C.; Rahuel, J.; Schoepfer, J.; Fretz, H. Structure-based design and synthesis of high affinity tripeptide ligands of the Grb2-SH2 domain. *J. Med. Chem.* **1998**, *41*, 3442−3449.

(15) Nam, J.-Y.; Kim, H.-K.; Son, K.-H.; Kim, S.-U.; Kwon, B.-M.; Han, M. Y.; Chung, Y. J.; Bok, S. H. Actinomycin D, C2 and VII, inhibitors of Grb2 Shc interaction produced by Streptomyces. *Bioorg. Med. Chem. Lett.* **1998**, *8*, 2001−2002.

(16) Burke, T. R., Jr.; Luo, J.; Yao, Z.-J.; Gao, Y.; Zhao, H.; Milne, G. W. A.; Guo, R.; Voigt, J. H.; King, C. R.; Yang, D. Monocarboxylic-based phosphotyrosyl mimetics in the design of Grb2 SH2 domain inhibitors. *Bioorg. Med. Chem. Lett.* **1999**.

(17) Alvi, K. A.; Pu, H.; Luche, M.; Rice, A.; App, H.; McMahon, G.; Dare, H.; Margolis, B. Asterriquinones produced by Aspergillus candidus inhibit binding of the Grb-2 adapter to phosphorylated EGF receptor tyrosine kinase. *J. Antibiot.* **1999**, *52*, 215−223.

(18) Ettmayer, P.; France, D.; Gounarides, J.; Jarosinski, M.; Martin, M. S.; Rondeau, J. M.; Sabio, M.; Topiol, S.; Weidmann, B.; Zurini, M.; Bair, K. W. Structural and conformational requirements for high- affinity binding to the SH2 domain of Grb2. *J. Med. Chem.* **1999**, *42*, 971−980.

(19) Schoepfer, J.; Fretz, H.; Gay, B.; Furet, P.; Garcia-Echeverria, C.; End, N.; Caravatti, G. Highly potent inhibitors of the Grb2-SH2 domain. *Bioorg. Med. Chem. Lett.* **1999**, *9*, 221−226.

(20) Furet, P.; Garcia-Echeverria, C.; Gay, B.; Schoepfer, J.; Zeller, M.; Rahuel, J. Structure-based design, synthesis, and X-ray crystallography of a high-affinity antagonist of the Grb2- SH2 domain containing an asparagine mimetic. *J. Med. Chem.* **1999**, *42*, 2358−2363.

(21) Hart, C. P.; Martin, J. E.; Reed, M. A.; Keval, A. A.; Pustelnik, M. J.; Northrop, J. P.; Patel, D. V.; Grove, J. R. Potent inhibitory ligands of the GRB2 SH2 domain from recombinant peptide libraries. *Cell. Signalling* **1999**, *11*, 453−464.

(22) Kim, H. K.; Nam, J. Y.; Han, M. Y.; Lee, E. K.; Choi, J. D.; Bok, S. H.; Kwon, B. M. Actinomycin D as a novel SH2 domain ligand inhibits Shc/Grb2 interaction in B104−1−1 (Neu*-transformed NIH3T3) and SAA (HEGFR-overexpressed NIH3T3) cells. *FEBS Lett.* **1999**, *453*, 174−178.

(23) Burke, T. R., Jr.; Yao, Z.-J.; Smyth, M. S.; Ye, B. Phosphotyrosyl-based motifs in the structure-based design of protein-tyrosine kinase-dependent signal transduction inhibitors. *Curr. Pharm. Des.* **1997**, *3*, 291−304.

(24) Burke, T. R., Jr; Gao, Y.; Yao, Z. J. In *Biomedical Chemistry: Applying Chemical Principles to the Understanding and Treatment of Disease*; Torrence, P., Ed.; John Wiley and Sons: New York, 2000; pp 189−210.

(25) Rahuel, J.; Gay, B.; Erdmann, D.; Strauss, A.; Garcia-Echeverria, C.; Furet, P.; Caravatti, G.; Fretz, H.; Schoepfer, J.; Grutter, M. G. Structural basis for specificity of GRB2−SH2 revealed by a novel ligand binding mode. *Nature Struct. Biol.* **1996**, *3*, 586−589.

(26) McNemar, C.; Snow, M. E.; Windsor, W. T.; Prongay, A.; Mui, P.; Zhang, R. M.; Durkin, J.; Le, H. V.; Weber, P. C. Thermodynamic and structural analysis of phosphotyrosine polypeptide binding to Grb2-SH2. *Biochemistry* **1997**, *36*, 10006−10014.
(27) Ogura, K.; Tsuchiya, S.; Terasawa, H.; Yuzawa, S.; Hatanaka, H.; Mandiyan, V.; Schlessinger, J.; Inagaki, F. Conformation of an Shc-derived phosphotyrosine-containing peptide complexed with the Grb2 SH2 domain. *J. Biomol. NMR* **1997**, *10*, 273−278.
(28) Ogura, K.; Tsuchiya, S.; Terasawa, H.; Yuzawa, S.; Hatanaka, H.; Mandiyan, V.; Schlessinger, J.; Inagaki, F. Solution structure of the SH2 domain of Grb2 complexed with the Shc-derived phosphotyrosine-containing peptide. *J. Mol. Biol.* **1999**, *289*, 439−445.
(29) Marseigne, I.; Roques, B. P. Synthesis of new amino acids mimicking sulfated and phosphorylated tyrosine residues. *J. Org. Chem.* **1988**, *53*, 3621−3624.
(30) Burke, T. R., Jr.; Smyth, M.; Nomizu, M.; Otaka, A.; Roller, P. P. Preparation of fluoro- and hydroxy-4-phosphonomethyl-D,L-phenylalanine suitably protected for solid-phase synthesis of peptides containing hydrolytically stable analogues of O-phosphotyrosine. *J. Org. Chem.* **1993**, *58*, 1336−1340.
(31) Ye, B.; Burke, T. R., Jr. L−O-Malonyltyrosine (L-OMT) a New Phosphotyrosyl Mimetic Suitably Protected for Solid-Phase Synthesis of Signal Transduction Inhibitory Peptides. *Tetrahedron Lett.* **1995**, *36*, 4733−4736.
(32) Miller, M. J.; Anderson, K. S.; Braccolino, D. S.; Cleary, D. G.; Gruys, K. J.; Han, C. Y.; Lin, K.-C.; Pansegrau, P. D.; Ream, J. E.; Sammons, R. D.; Sikorski, J. A. EPSP synthase inhibitor design II. The importance of the 3-phosphate group for ligand binding at the shikimate-3-phosphate site & the identification of 3-malonate ethers as novel 3-phosphate mimetics. *Bioorg. Med. Chem. Lett.* **1993**, *7*, 1435−1440.
(33) Burke, T. R., Jr.; Russ, P.; Lim, B. Preparation of 4-[bis(*tert*-butyl)phosphonomethyl]-N−Fmoc-DL-phenylalanine; a hydrolytically stable analogue of O-phosphotyrosine potentially suitable for peptide synthesis. *Synthesis* **1991**, *11*, 1019−1020.
(34) Yao, Z. J.; Gao, Y.; Voigt, J. H.; Ford, H.; Burke, T. R. Synthesis of Fmoc-protected 4-carboxydifluoromethyl-L-phenylalanine: A phosphotyrosyl mimetic of potential use for signal transduction studies. *Tetrahedron* **1999**, *55*, 2865−2874.
(35) Yao, Z. J.; Gao, Y.; Burke, T. R., Jr. Preparation of (L)-*N* α-Fmoc-4-[di-(*tert*-butyl) phosphonomethyl]phenylalanine from L-tyrosine. *Tetrahedron Assym.* **1999**, *10*, 3727−3734.
(36) Gao, Y.; Burke, T. R., Jr. Stereoselective preparation of 1-4-(2′-malonyl)phenylalanine suitably protected for Fmoc-based synthesis of potent signal transduction inhibitor ligands. *Synlett* **2000**, 134−136.
(37) Burke, T. R.; Ye, B.; Akamatsu, M.; Ford, H.; Yan, X. J.; Kole, H. K.; Wolf, G.; Shoelson, S. E.; Roller, P. P. 4′-O-[2-(2-fluoromalonyl)]-L-tyrosine: A phosphotyrosyl mimic for the preparation of signal transduction inhibitory peptides. *J. Med. Chem.* **1996**, *39*, 1021−1027.
(38) Burke, T. R., Jr.; Yao, Z.-J.; Luo, J. H.; Gao, Y.; Voigt, J.; King, C. R.; Yang, D. Non-phosphate-containing phosphotyrosyl mimetics and their use in signal transduction studies. *Abstracts of Papers*, 217th National Meeting of the American Chemical Society, Anaheim, CA, March 21−25, 1999; American Chemical Society: Washington, DC, 1999; MEDI 149.
(39) Burke, T. R., Jr.; Luo, J.; Yao, Z.-J.; Gao, Y.; Milne, G. W. A.; Guo, R.; Voigt, J. H.; King, C. R.; Yang, D. Monocarboxylic phosphotyrosyl mimetics in the design of Grb2 SH2 domain inhibitors. *Bioorg. Med. Chem. Lett.* **1999**, *9*, 347−352.
(40) Tong, L.; Warren, T. C.; Lukas, S.; SchembriKing, J.; Betageri, R.; Proudfoot, J. R.; Jakes, S. Carboxymethyl-phenylalanine as a replacement for phosphotyrosine in SH2 domain binding. *J. Biol. Chem.* **1998**, *273*, 20238−20242.
(41) Lowenstein, E. J.; Daly, R. J.; Batzer, A. G.; Li, W.; Margolis, B.; Lammers, R.; Ullrich, A.; Skolnik, E. Y.; Barsagi, D.; Schlessinger, J. The SH2 and SH3 Domain-Containing Protein GRB2 Links Receptor Tyrosine Kinases to Ras Signaling. *Cell* **1992**, *70*, 431−442.
(42) Molecular Simulations Inc., San Diego, CA.

JM9904248